Matrix Infrared Spectra and Density Functional Calculations of $Ni(CO)_x^-$, $x = 1-3$

Mingfei Zhou and Lester Andrews*

Contribution from the Department of Chemistry, University of Virginia, Charlottesville, Virginia 22901

Received June 15, 1998

Abstract: Laser-ablated Ni atoms and electrons react with CO in excess argon during condensation to form the $Ni(CO)_{1-4}$ complexes and $Ni(CO)_{1-3}^-$ anions. Matrix infrared spectra of the neutral complexes with $^{12}C^{16}O$, $^{13}C^{16}O$, and $^{12}C^{18}O$ substitution are in agreement with earlier reports with thermal Ni atoms. In addition, new absorptions at 1847.0, 1801.7, and 1858.8 cm^{-1} exhibit isotopic spectra in excellent agreement with DFT calculations for the $Ni(CO)_{1-3}^-$ anions. An experiment doped with the CCl_4 electron-trapping molecule gave the same $Ni(CO)_{1-4}$ spectrum without the corresponding anions, which strongly supports this identification of the molecular anions.

Introduction

Unsaturated transition metal carbonyls are important in processes such as organometallic synthesis and homogeneous catalysis and photodecomposition of organometallics.[1] In particular, the metal monocarbonyls are often considered as models for CO binding to the metal surface.[2] Although the neutral nickel carbonyls have been well studied both by experiment[3] and theory,[4] there is relatively little work on the anions. The $Ni(CO)_x^-$ ($x = 1-3$) anions have been observed in the negative ion mass spectrum of $Ni(CO)_4$ and examined by photodetachment and collision-induced dissociation methods.[5−7] Only $Ni(CO)_3^-$ has been characterized by photodissociation in ion cyclotron resonance[8] and by vibrational spectroscopy in a matrix isolation study.[9] Here we report the infrared spectra and density functional calculations of $Ni(CO)_x^-$ ($x = 1-3$), which are prepared by reactions of laser-ablated nickel atoms and electrons with CO in excess argon.

Experimental and Computational Methods

Pulsed-laser ablation of nickel is used for the present matrix isolation study.[10] In contrast to a thermal atom source,[3] electrons are produced in the laser-ablation process and anions can also be formed via electron capture by neutral molecules during condensation.[10−12] Density functional calculations are done for band identification, using the Gaussian 94 program,[13] BP86 functional,[14] 6-311+G* basis sets for C and O atoms,[15] and the all-electron set of Wachters and Hay as modified by Gaussian 94 for nickel.[16]

Results and Discussion

The product absorptions for laser-ablated nickel atom reactions with CO in Ar are shown in Figures 1 and 2 and listed in Table 1. Also given are frequencies for the ^{13}CO and $C^{18}O$ isotopic modifications and mixtures with normal CO. The NiCO absorption was observed at 1994.4 cm^{-1} after deposition, and $Ni(CO)_{2,3,4}$ bands were produced on annealing, in agreement with earlier works.[3]

NiCO. The 1994.4 cm^{-1} observation for NiCO is in excellent agreement with the 2006.2 cm^{-1} DFT/BP86 prediction for the ground $^1A_1$ state NiCO complex. Note that the 12/13 ratio, 1.02466, exceeds the ratio for CO itself, 1.02248, and the 16/18 ratio, 1.02099, is less than the CO ratio, 1.02444. This means that on binding to Ni, the form of the normal mode for the C−O vibration changes to involve more C and less O motion as

(1) Tumas, W.; Gitlin, B.; Rosan, A. M.; Yardley, J. T. *J. Am. Chem. Soc.* **1982**, *104*, 55.
(2) Walsh, S. P.; Goddard, W. A., III *J. Am. Chem. Soc.* **1976**, *98*, 7908.
(3) (a) DeKock, R. L. *Inorg. Chem.* 1971, *10*, 1205. (b) Kündig, E. P.; McIntosh, D.; Moskovits, M.; Ozin, G. A. *J. Am. Chem. Soc.* **1973**, *95*, 7234. (c) Bach, S. B. H.; Taylor, C. A.; Van Zee, R. J.; Vala, M. T.; Weltner, W., Jr. *J. Am. Chem. Soc.* **1986**, *108*, 7104. (d) Joly, H. A.; Manceron, L. *Chem. Phys.* **1998**, *226*, 61.
(4) Howard, I. A.; Pratt, G. W.; Johnson, K. H.; Dresselhaus, G. *J. Chem. Phys.* **1981**, *74*, 3415. Burdett, J. K. *Inorg. Chem.* **1975**, *14*, 375; Jonas, V.; Thiel, W. *J. Chem. Phys.* **1995**, *102*, 8474. Fournier, R. *J. Chem. Phys.* **1993**, *99*, 1801. Blomberg, M.; Brandemark, U.; Johanson, J.; Siegbahn, P.; Wennerberg, J. *J. Chem. Phys.* **1988**, *88*, 4324. Blomberg, M. R. A.; Siegbahn, P. E. M.; Lee, T. J.; Rendell, A. P.; Rice, J. E. *J. Chem. Phys.* **1991**, *95*, 5898. Sodupe, M.; Bauschlicher, C. W., Jr.; Lee, T. J. *Chem. Phys. Lett.* **1992**, *189*, 266.
(5) Compton, R. N.; Stockdale, J. A. D. *Int. J. Mass Spectrom. Ion Phys.* **1976**, *22*, 47.
(6) Stevens, A. E.; Feigerle, C. S.; Lineberger, W. C. *J. Am. Chem. Soc.* **1982**, *104*, 5026.
(7) Sunderlin, L. S.; Wang, D.; Squires, R. R. *J. Am. Chem. Soc.* **1993**, *115*, 12060.
(8) Dunbar, R. C.; Hutchinson, B. B. *J. Am. Chem. Soc.* **1974**, *96*, 3816.
(9) Breeze, P. A.; Burdett, J. K.; Turner, J. J. *Inorg. Chem.* **1981**, *20*, 3369.
(10) (a) Kang, H.; Beauchamp, J. L. *J. Phys. Chem.* **1985**, *89*, 3364. (b) Burkholder, T. R.; Andrews, L. *J. Chem. Phys.* **1991**, *95*, 8697. (c) Hassanzadeh, P.; Andrews, L. *J. Phys. Chem.* **1992**, *96*, 9177. (d) Citra, A.; Chertihin, G. V.; Andrews, L.; Neurock, M. *J. Phys. Chem. A* **1997**, *101*, 3109.
(11) Chertihin, G. V.; Andrews L. *J. Chem. Phys.* **1998**, *108*, 6404.
(12) Andrews, L.; Zhou, M.; Willson, S. P.; Kushto, G. P.; Snis, A.; Panas, I. *J. Chem. Phys.* **1998**, *109*, 177.
(13) *Gaussian 94, Revision B.1*. Frisch, M. J.; Trucks, G. W.; Schlegel, H. B.; Gill, P. M. W.; Johnson, B. G.; Robb, M. A.; Cheeseman, J. R.; Keith, T.; Petersson, G. A.; Montgomery, J. A.; Raghavachari, K.; Al-Laham, M. A.; Zakrzewski, V. G.; Ortiz, J. V.; Foresman, J. B.; Cioslowski, J.; Stefanov, B. B.; Nanayakkara, A.; Challacombe, M.; Peng, C. Y.; Ayala, P. Y.; Chen, W.; Wong, M. W.; Andres, J. L.; Replogle, E. S.; Gomperts, R.; Martin, R. L.; Fox, D. J.; Binkley, J. S.; Defrees, D. J.; Baker, J.; Stewart, J. P.; Head-Gordon, M.; Gonzalez, C.; Pople J. A. Gaussian, Inc.: Pittsburgh, PA, 1995.
(14) Perdew, J. P. *Phys. Rev. B* **1986**, *33*, 8822; Becke, A. D. *J. Chem. Phys.* **1993**, *98*, 5648.
(15) McLean, A. D.; Chandler, G. S. *J. Chem. Phys.* **1980**, *72*, 5639. Krishnan, R.; Binkley, J. S.; Seeger, R.; Pople, J. A. *J. Chem. Phys.* **1980**, *72*, 650.
(16) Wachters, H. J. H. *J. Chem. Phys.* **1970**, *52*, 1033. Hay, P. J. *J. Chem. Phys.* **1977**, *66*, 4377.

10.1021/ja9820644 CCC: $15.00
Published on Web 10/17/1998

Table 1. Infrared Absorptions (cm^{-1}) from Co-deposition of Laser Ablated Nickel Atoms with Carbon Monoxide in Excess Argon at 10 K

$^{12}C^{16}O$	$^{13}C^{16}O$	$^{12}C^{18}O$	$^{12}C^{16}O + ^{13}C^{16}O$	$^{12}C^{16}O + ^{12}C^{18}O$	*R*(12/13)	*R*(16/18)	assignment
2138.1	2091.1	2087.1			1.02248	1.02444	CO
2071.5	2022.4	2027.4	2071.5, 2051.9, 2022.4	2071.5, 2053.8, 2027.4	1.02428	1.02175	$Ni(CO)_2$
2051.2	2004.9	2004.3	2051.3, 2032.6, 2021.3, 2012.6, 2004.9	2051.2, 2033.1, 2021.5, 2012.5, 2004.3	1.02309	1.02340	$Ni(CO)_4$
2032.3	1986.4	1985.9			1.02311	1.02336	$(N_2)Ni(CO)_3$
2031.7	1985.7	1985.2			1.02317	1.02342	site
2017.2	1971.9	1970.7	2017.2, 1996.0, 1982.7, 1971.8	2017.2, 1996.3, 1982.2, 1970.6	1.02297	1.02360	$Ni(CO)_3$
1994.4	1946.4	1953.4	1994.3, 1946.3	1994.3, 1953.3	1.02466	1.02099	NiCO
1991.6	1943.5	1950.5	1991.4, 1943.5	1991.4, 1950.5	1.02475	1.02107	NiCO site
1965.5	1921.2	1920.6	1965.5, 1938.3, 1921.2	1965.5, 1938.6, 1920.5	1.02306	1.02338	$Ni(CO)_2$
1863.6	1823.3		1863.4, 1823.3		1.02210		HCO
1858.8	1815.1	1819.0	1858.7, 1839.2, 1825.9, 1815.2	1858.8, 1841.7, 1829.3, 1818.9	1.02408	1.02188	$Ni(CO)_3^-$
1853.8	1810.2	1814.3	1853.8, 1834.5, 1821.2, 1810.2	1853.8, 1836.9, 1824.7, 1814.3	1.02409	1.02177	$Ni(CO)_3^-$ site
1850.1	1805.1	1813.2	1850.1, 1805.1	1850.1, 1813.2	1.02497	1.02033	$NiCO^-$ site
1847.0	1802.0	1810.2	1847.0, 1802.0	1847.0, 1810.2	1.02497	1.02033	$NiCO^-$
1801.7	1759.8	1762.4	1801.7, 1775.6, 1760.0	1801.6, 1778.3, 1762.6	1.02381	1.02230	$Ni(CO)_2^-$
1515.5	1482.2	1479.5	1515.5, 1497.4, 1482.2	1515.5, 1497.4, 1479.5	1.02247	1.02433	$(CO)_2^-$
515.5	510.6	505.3	515.4, 513.4, 510.5	515.4, 511.6, 505.2	1.00960	1.02019	$^{58}Ni(CO)_2$
514.4	509.7	504.1			1.00922	1.02043	site
512.0	507.1	501.7			1.00966	1.02053	$^{60}Ni(CO)_2$
510.8	505.8				1.00989		site
464.6	448.6	457.3			1.03567	1.01596	$Ni(CO)_4$
458.4	451.3	451.6	458.3, 456.5, 455.0(b), 452.3, 451.4	458.4, 457.9, 456.2, 454.7, 453.1, 451.6	1.01573	1.01506	$^{58}Ni(CO)_3$
455.3	448.4	448.4			1.01539	1.01539	$^{60}Ni(CO)_3$
434.6	428.8	428.3	434.5, 433.2, 431.4, 430.1, 428.8		1.01353	1.01471	$^{58}Ni(CO)_4$
433.3	427.6	426.8			1.01333	1.01523	site
431.5	425.7	425.1			1.01362	1.01506	$^{60}Ni(CO)_4$
430.1	424.5	423.6			1.01319	1.01534	site

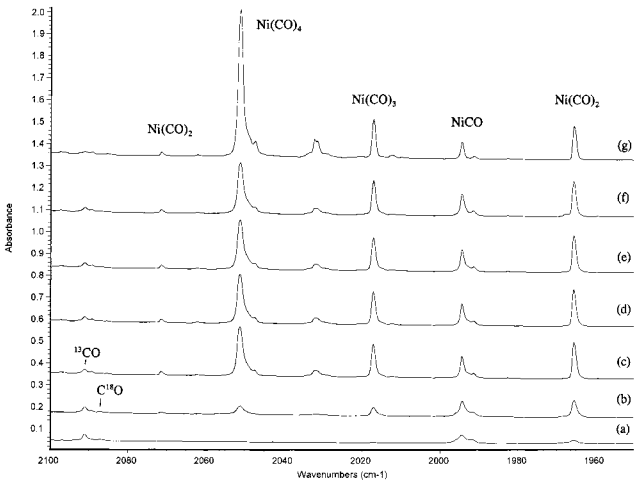

Figure 1. Infrared spectra in the 2100−1950 cm^{-1} region for laser-ablated Ni atoms co-deposited with 0.4% CO in argon at 10 ± 1 K: (a) sample co-deposited for 1.5 h, (b) after 20 K annealing, (c) after 25 K annealing, (d) after 850−1000 nm photolysis, (e) after 630−1000 nm photolysis, (f) after 470−1000 nm photolysis, and (g) after 30 K annealing. The weak ^{13}CO and $C^{18}O$ bands are in natural abundance.

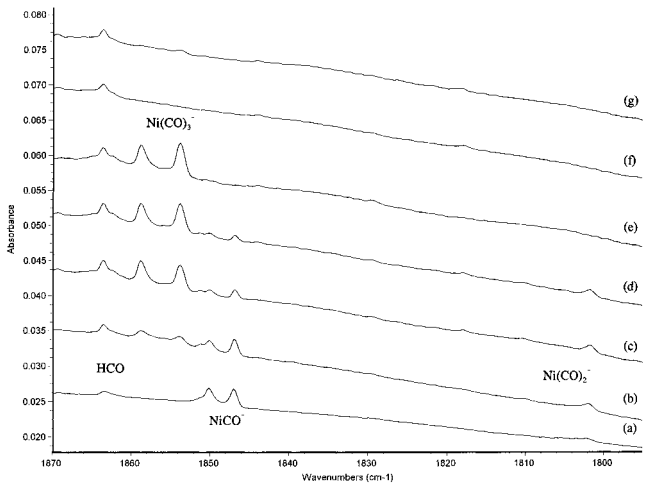

Figure 2. Infrared spectra in the 1870−1795 cm^{-1} region for laser-ablated Ni atoms co-deposited with 0.4% CO in argon at 10 ± 1 K: (a) sample co-deposited for 1.5 h, (b) after 20 K annealing, (c) after 25 K annealing, (d) after 850−1000 nm photolysis, (e) after 630−1000 nm photolysis, (f) after 470−1000 nm photolysis, and (g) after 30 K annealing.

carbon vibrates "antisymmetrically" between Ni and C atoms. Joly and Manceron have most recently observed NiCO at 1994.5 cm^{-1} from thermal Ni atom reactions, and noted the substantial vibrational coupling between the Ni−C and C−O bond stretching coordinates.[3d]

$Ni(CO)_2$. The $Ni(CO)_2$ molecule is bent instead of the linear structure suggested[3a] from observation of only the strong antisymmetric C−O vibration at 1965.5 cm^{-1} since the symmetric stretching mode is observed here as a weak 2071.5 cm^{-1} band. Note the matching asymmetries in the mixed isotopic intermediate band positions (Table 1): the symmetric mode for $Ni(^{12}CO)(^{13}CO)$ is 5.0 cm^{-1} *above* the pure isotopic mean and the antisymmetric mode is 5.0 cm^{-1} *below* the pure isotopic mean while this asymmetry for both modes of $Ni(C^{16}O)(C^{18}O)$ is 4.4 cm^{-1} due to interaction between these two modes for the mixed isotopic molecule. The matching isotopic band asymmetries verify assignment of the weaker symmetric mode to the same molecule as the stronger antisymmetric mode.

DFT calculations predict a bent complex with a 171° C−Ni−C bond angle and carbonyl stretching modes at 1987.6 and 2066.5 cm^{-1}. Not only is the linear structure 2.7 kcal/mol higher in energy, it has one imaginary bending frequency, and is therefore not a stable structure. This suggests that the bent equilibrium structure is not due to the matrix. The calculated frequencies are 22.1 cm^{-1} higher and 5.0 cm^{-1} lower than the observed values, which is very good agreement. Of more importance notice the excellent agreement between the observed and calculated isotopic frequency ratios for the antisymmetric and symmetric C−O stretching modes, which are slightly

Table 2. Geometries, Frequencies (cm^{-1}), Intensities (km/mol), and Isotopic Frequency Ratios Calculated (BP86/6-311+G*) for NiCO, $NiCO^-$ and $NiCO^+$

molecule	geometry	$^{12}C^{16}O$	$^{13}C^{16}O$	$^{12}C^{18}O$	*R*(12/13)	*R*(16/18)
NiCO[a]	Ni−C: 1.675 Å	348.1(10)	337.6(9)	344.1(10)	1.0311	1.0116
($^1\Sigma$)	C−O: 1.167 Å	602.9(1)	597.3(1)	586.9(1)	1.0094	1.0273
	∠NiCO: 180°	2006.2(554)	1956.6(525)	1965.3(534)	1.0254	1.0208
NiCO	Ni−C: 1.859 Å	245.7(28)	241.3(27)	239.5(26)	1.0182	1.0259
($^3A'$)	C−O: 1.162 Å	453.6(10)	442.9(8)	447.8(10)	1.0242	1.0130
	∠NiCO: 145.9°	1946.3(922)	1902.3(878)	1900.3(884)	1.0231	1.0242
$NiCO^-$	Ni−C: 1.691 Å	200.6(77)	194.6(73)	198.2(75)	1.0308	1.0121
($^2\Sigma$)	C−O: 1.188 Å	575.7(5)	570.4(4)	560.2(5)	1.0093	1.0277
	∠NiCO: 180°	1870.2(792)	1823.6(761)	1832.6(748)	1.0256	1.0205
$NiCO^+$	Ni−C: 1.818 Å	305.5(0.2)	296.5(0.3)	301.6(0.2)	1.0304	1.0129
($^2\Sigma$)	C−O: 1.135 Å	441.3(4)	436.5(4)	430.7(3)	1.0110	1.0246
	∠NiCO: 180°	2173.7(188)	2123.4(176)	2124.0(185)	1.0237	1.0234

[a] The $^1\Sigma$ state is 35.3 kcal/mol lower in energy than the $^3A'$ state.

Table 3. Geometries, Frequencies (cm^{-1}), and Intensities (km/mol) Calculated (BP86/6-311+G*) for the $Ni(CO)_2$ Molecule and $Ni(CO)_2^-$ Anion

molecule	rel energy	geometry (D, deg)	frequency (intensity)
$Ni(CO)_2$	0	Ni−C: 1.767 Å, C−O: 1.158 Å	a_1: 60.8(2), a_2: 296.2(0), b_2: 302.7(1),
$^1A_1$		∠CNiC: 142.2°, ∠NiCO: 171.1°	b_1: 379.3(4), a_1: 453.7(3), a_1: 479.7(1),
			b_2: 527.3(82), b_2: 1987.6(1674), a_1: 2066.5(94)
$Ni(CO)_2$	+2.7	Ni−C: 1.784 Å, C−O: 1.154 Å	π_u: −99.5(7), π_g: 299.6(0), π_u: 305.8(13),
$^1\Sigma_g$		∠CNiC: 180°, ∠NiCO: 180°	Σ_g: 438.2(0), Σ_g: 506.9(462), Σ_u: 1994.0(2101),
			Σ_g: 2093.2(0)
$Ni(CO)_2^-$	−19.9	Ni−C: 1.756 Å, C−O: 1.188 Å	a_1: 57.7(2), b_1: 274.1(484), a_2: 313.4(0),
$^2A_1$		∠CNiC: 152.4°, ∠NiCO: 177.1°	b_2: 355.8(5), a_1: 401.1(40), a_1: 472.7(0),
			b_2: 519.1(1), b_2: 1813.9(2148), a_1: 1866.1(489)
$Ni(CO)_2^-$	−19.3	Ni−C: 1.763 Å, C−O: 1.189 Å	−63.4(1), −49.0(4), 302.8(14), 310.0(0),
(doublet)		∠CNiC: 180°, ∠NiCO: 180°	368.1(0), 368.8(23),453.9(0), 490.5(1),
			1803.3(2462), 1874.2(0)

Table 4. Comparison of Observed and Calculated Isotopic Frequency Ratios for C−O Stretching Fundamentals of the $Ni(CO)_2$ Molecule and $Ni(CO)_2^-$ Anion

molecule	vibrational mode	*R*(12/13 obsd)	*R*(12/13 calcd)	*R*(16/18 obsd)	*R*(16/18 calcd)
$Ni(CO)_2$	antisym	1.02306	1.02364	1.02338	1.02332
	sym	1.02428	1.02469	1.02175	1.02181
$Ni(CO)_2^-$	antisym	1.02381	1.02451	1.02230	1.02209
	sym	not obsd	1.02544	not obsd	1.02084

Table 5. Calculated (BP86/6-311+G*) Geometry, C−O Stretching Vibrational Frequencies (cm^{-1}), Intensities (km/mol), and Isotopic Frequency Ratios for the Doublet $Ni(CO)_3^-$ Anion[a]

mode	$^{12}C^{16}O$	$^{13}C^{16}O$	$^{12}C^{18}O$	*R*(12/13)	*R*(16/18)
antisym	1848.5(1785)	1804.1(1705)	1808.7(1704)	1.02461	1.02200
sym	1920.4(0)	1873.9(0)	1879.7(0)	1.02481	1.02165

[a] Structure: Ni−C, 1.777 Å; C−O, 1.181 Å; ∠CNiC, 120°; ∠NiCO, 180°; D_{3h} symmetry.

different (Table 4). The symmetric mode has more carbon and less oxygen motion as compared to the antisymmetric mode, but both of these modes are slightly different from the C−O mode in NiCO, based on the isotopic frequency ratios.

$Ni(CO)_3$ and $Ni(CO)_4$. The $Ni(CO)_3$ and $Ni(CO)_4$ absorptions at 2017.2 and 2051.2 cm^{-1} increase markedly on annealing in agreement with previous work.[3] Note that the 12/13 and 16/18 isotopic frequency ratios for these bands (Table 1) are comparable to those for the antisymmetric C−O mode for $Ni(CO)_2$. The mixed isotopic spectra are quartets with 2:1:1:2 relative intensities for $Ni(CO)_3$ and are quintets with 8:2:3:2:8 relative intensities for $Ni(CO)_4$. These band profiles are characteristic of doubly degenerate vibrations for trigonal and triply degenerate vibrations for tetrahedral molecules, respectively.[17] The weaker 2032.3 cm^{-1} band that also grows in on annealing has been attributed to the $(N_2)Ni(CO)_3$ complex.[3b]

$NiCO^-$. Compared with thermal nickel atom reactions, several new absorptions are observed with laser ablation. Figure 2 shows spectra in the 1870−1795 cm^{-1} region of particular interest here. Sharp bands at 1850.1 and 1847.0 cm^{-1} and weak bands at 1801.7 and 1863.6 cm^{-1} (due to HCO)[18] were observed after deposition. New 1810.2, 1858.8, and 1853.8 cm^{-1} bands appear on annealing to 20 and 25 K. The multiplet structure in the $C^{16}O + C^{18}O$ mixed isotopic spectra are illustrated in Figure 3.

The new 1850.1, 1847.0 cm^{-1} matrix site bands shifted to 1805.1, 1802.0 cm^{-1} with $^{13}C^{16}O$ to 1813.2, 1810.2 cm^{-1} with $^{12}C^{18}O$. These two bands, like those for the NiCO molecule, exhibit larger carbon isotopic and smaller oxygen isotopic ratios than CO, which indicates more carbon participation in this vibrational motion between oxygen and another mass. The isotopic doublet structure observed in both mixed $^{12}CO + {}^{13}CO$

(17) Darling, J. H.; Ogden, J. S. *J. Chem. Soc., Dalton Trans.* **1972**, 2496.

(18) Milligan, D. E.; Jacox, M. E. *J. Chem. Phys.* **1969**, *51*, 277. Hydrogen atoms, from dissociation of trace water impurity, react with CO.

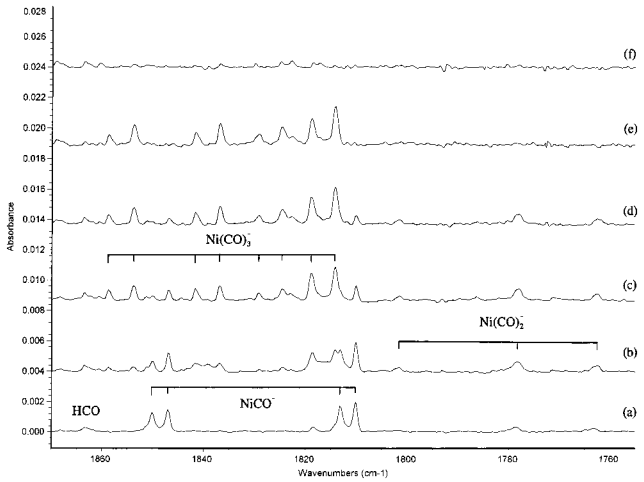

Figure 3. Infrared spectra in the 1870−1755 cm^{-1} region for laser-ablated Ni atoms co-deposited with 0.6% $^{12}C^{16}O + {}^{12}C^{18}O$ mixture in argon at 10 ± 1 K: (a) sample co-deposited for 1.5 h, (b) after 20 K annealing, (c) after 25 K annealing, (d) after 850−1000 nm photolysis, (e) after 630−1000 nm photolysis, and (f) after 470−1000 nm photolysis.

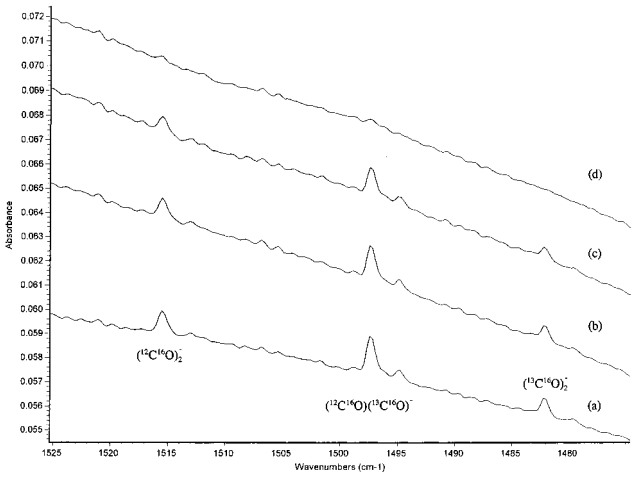

Figure 4. Infrared spectra in the 1525−1475 cm^{-1} region for laser ablated nickel co-deposited with 0.4% CO in argon at 10 ± 1 K: (a) sample co-deposited for 1.5 h, (b) after 850−1000 nm photolysis, (c) after 630−1000 nm photolysis, and (d) after 470−1000 nm photolysis.

and $C^{16}O + C^{18}O$ experiments comfirms that only one CO subunit is involved. The 1850.1, 1847.0 cm^{-1} bands are assigned to the C−O stretching vibration of the $NiCO^-$ anion in different matrix sites. The DFT calculation predicts that $NiCO^-$ has a $^2\Sigma$ ground state, with a C−O stretching vibration at 1870.2 cm^{-1}, and isotopic frequency ratios in very good agreement with experiment, as shown in Table 2. Note that both calculations and experiment show slightly higher 12/13 and lower 16/18 ratios for $NiCO^-$ than for NiCO. Clearly the DFT/BP86 calculations correctly model this subtle difference in the potential surfaces between NiCO and $NiCO^-$. Finally, this calculation predicted the C−O fundamental for NiCO to be 11.8 cm^{-1} too high and for the $NiCO^-$ anion 23.2 cm^{-1} too high, which provides a calibration for the frequency calculations.

$Ni(CO)_2^-$. The 1801.7 cm^{-1} band increases on early annealing at the expense of $NiCO^-$, and is assigned to the antisymmetric vibration of the $Ni(CO)_2^-$ anion, based on the 1/2/1 triplet isotopic structure observed in mixed isotopic experiments (Figure 3), which denotes two equivalent CO subgroups, as well as the results of DFT calculations. Like the neutral dicarbonyl, the linear dicarbonyl anion is higher in energy and has imaginary bending frequencies. The $Ni(CO)_2^-$ anion also has a slightly bent ground state. The calculated antisymmetric stretching vibration at 1813.9 cm^{-1} and the isotopic frequency ratios are in excellent agreement with the observed values. Again, there is slightly more carbon participation for the anion than the neutral dicarbonyl complex. The symmetric vibration calculated at 1866.1 cm^{-1} is not observed here due to lower intensity.

$Ni(CO)_3^-$. The 1858.8, 1853.8 cm^{-1} bands were only observed after annealing. In the mixed isotopic sample, quartets with two weaker intermediate components were observed for both bands (Figure 3), so three equivalent CO submolecules are involved in this doubly degenerate vibration.[9,17] These two bands are due to the $Ni(CO)_3^-$ molecular anion. The 1858.8 cm^{-1} band has been assigned to $Ni(CO)_3^-$ from matrix vacuum−UV photolysis of $Ni(CO)_4$.[9] The DFT calculation also supports this assignment: $Ni(CO)_3^-$ has a $^2A_2''$ doublet ground state with D_{3h} symmetry and a calculated antisymmetric vibration of 1848.5 cm^{-1}, which is in excellent agreement with the experimental observations.

No evidence was found here for $NiCO^+$, which is calculated to absorb at 2173.7 cm^{-1}, which is above CO. Unfortunately, $Ni^{13}CO^+$ is probably masked by ^{12}CO in the sample, and we cannot provide convincing evidence for $NiCO^+$. The counterion for the anions in these experiments is likely the Ni^+ cation,[10a] but $NiCO^+$ is probably present as well.

The $Ni(CO)_x^-$, $x = 1-3$, vibrational frequencies were red shifted 147.4, 163.8, and 158.4 cm^{-1}, respectively, compared with the corresponding neutral $Ni(CO)_x$ molecules, and they appeared just above the region expected for vibrations of bridged carbonyls. However, bridged metal cluster carbonyl species can be ruled out due to the relatively low laser power used here. Although the DFT calculated frequencies for bridged Ni_2CO and $Ni_2(CO)_2$ species lie in this region, the isotopic frequency ratios are quite different from the $Ni(CO)_x^-$ anion ratios calculated and observed here.

In addition, very weak bands appear on annealing at 1818.0, 1829.0, and 1869.4 cm^{-1}. These bands correspond to stronger bands observed in thermal experiments for higher $Ni_x(CO)_y$ species, which increase with increasing Ni atom concentrations.[3d] This observation confirms that Ni atoms dominate the present reaction system.

$(CO)_2^-$. A sharp, weak new metal-independent band was observed at 1515.5 cm^{-1}, and Figure 4 shows $^{12}CO + {}^{13}CO$ mixed isotopic spectra for this absorption. The weak 1515.5 cm^{-1} band decreases on annealing and on photolysis, and shows essentially diatomic CO isotopic ratios. The 1/2/1 triplet absorptions in mixed isotopic experiments verify the participation of two equivalent CO subunits in this normal mode. In addition the 1515.5 cm^{-1} band is observed in laser ablation experiments with CO and other metals.[19] The argon matrix band is just below the 1517.7 cm^{-1} neon matrix band assigned to $(CO)_2^-$.[20] Furthermore, extensive theoretical calculations have confirmed this matrix infrared identification of $(CO)_2^-$.[21] The observation of $(CO)_2^-$ in these experiments further demonstrates the presence of electrons in laser-ablation experiments.

CCl_4 Doping. A series of experiments was done with different laser powers and different concentrations of CCl_4 added to serve as an electron trap. Comparison is made to an

(19) Zhou, M. F.; Chertihin, G. V.; Andrews, L. *J. Chem. Phys.* In press (Fe + CO).

(20) Thompson, W. E.; Jacox, M. E. *J. Chem. Phys.* **1991**, *95*, 735.

(21) Thomas, J. R.; DeLeeuw, B. J.; O'Leary, P.; Schaefer, H. F., III; Duke, B. J.; O'Leary, B. *J. Chem. Phys.* **1995**, *102*, 6525.

experiment with 0.4% CO and the same low laser power as the experiment used for Figures 1 and 2, and 0.1% CCl_4 added to the argon matrix gas. The initial spectrum of the deposited sample was much the same as illustrated in Figure 1 showing NiCO, and annealing produced the $Ni(CO)_{2-4}$ absorptions, as before. However, the Figure 2 region contained only a weak ClCO band at 1877.0 cm^{-1},[22] and annealing failed to produce other absorptions in this region. Also, the 1515.5 cm^{-1} $(CO)_2^-$ band was absent from the spectrum. In addition, the lower region contained new bands at 1036.4 cm^{-1} for CCl_3^+, at 1019.3, 928.3, and 501.4 cm^{-1} for $Cl_2CCl-Cl$, and at 898.0 cm^{-1} for the CCl_3 radical.[23-26] Full arc photolysis had no effect on the $Ni(CO)_{1-4}$ absorptions, as found for other samples without CCl_4, but the CCl_3^+ and $Cl_2CCl-Cl$ bands were almost destroyed, while the CCl_3 absorption increased, in agreement with previous observations.[25,26] The removal of infrared absorptions from identical experiments upon doping with an electron trapping molecule adds further support to their identification as molecular anions.

Photochemistry. The absorptions assigned to $Ni(CO)_x^-$ anions exhibit selective photolysis behavior as shown in Figure 2. Filtered (glass and water) infrared photolysis (850−1000 nm) with a 500 W tungsten lamp reduced the $NiCO^-$ absorption about 40% with no effect on the $Ni(CO)_2^-$ and $Ni(CO)_3^-$ bands, but this radiation in the 630−1000 nm region totally destroyed the $NiCO^-$ and $Ni(CO)_2^-$ absorptions, while the 1853.8 cm^{-1} site band of $Ni(CO)_3^-$ increased about 20% with no change for the 1858.8 cm^{-1} site band. Continued photolysis in the 470−1000 nm region destroyed the $Ni(CO)_3^-$ absorptions, which is in agreement with the photodisappearance of $Ni(CO)_3^-$ when irradiated at 2.0−2.5 eV using the techniques of ion cyclotron resonance.[8] The matrix photolysis behavior is in accord with the low electron affinities for the neutral species derived from photoelectron spectra in the gas phase,[6] and provides further evidence to support the matrix identification of the $Ni(CO)_x^-$ anions.

The 1515.5 cm^{-1} $(CO)_2^-$ band is reduced 10% by 850−1000 nm radiation, reduced 50% at 630−1000 nm, and almost destroyed by 470−1000 nm photolysis. Comparison with the present matrix photolysis of $Ni(CO)_x^-$ species suggests a comparable electron photodetachment energy for $(CO)_2^-$, certainly more than $(CO)^-$, which has not been characterized.

Reaction Mechanisms. The $NiCO^-$ anions are formed by exothermic (0.80 ± 0.01 eV)[6] electron capture by NiCO molecules during co-deposition, reactions 1, with Ni atoms and

$$Ni + CO \rightarrow NiCO \quad (1a)$$

$$NiCO + e^- \rightarrow NiCO^- \quad (1b)$$

electrons from the laser ablation process. Since Ni^- is only a minor fragment in the negative ion mass spectrum[5] of $Ni(CO)_4$, and s^2d^9 ground-state Ni^- is not expected to bind CO,[6,7] the Ni^- reaction with CO probably does not contribute to the $NiCO^-$ observed here.

The $Ni(CO)_2^-$ and $Ni(CO)_3^-$ anions increased on annealing, like their neutral counterparts, and they are produced from reactions 2 and 3, which are also exothermic processes.[7] The

$$NiCO^- + CO \rightarrow Ni(CO)_2^- \quad (2)$$

$$Ni(CO)_2^- + CO \rightarrow Ni(CO)_3^- \quad (3)$$

1853.8 cm^{-1} site band of $Ni(CO)_3^-$ was not observed in the previous matrix experiments;[9] this band increases on 630−1000 nm photolysis when $NiCO^-$ and $Ni(CO)_2^-$ are bleached, suggesting that $Ni(CO)_3^-$ can also be formed by exothermic (1.08 ± 0.01 eV)[6] reaction 4.

$$Ni(CO)_3 + e^- \rightarrow Ni(CO)_3^- \quad (4)$$

The $(CO)_2^-$ anion absorbing here at 1515.5 cm^{-1} is probably formed through electron capture by a van der Waals CO dimer trapped in the matrix, reaction 5, since there is no evidence for a stable isolated CO^- anion. This reaction must also be an exothermic process based on the comparable matrix photochemistry of $(CO)_2^-$ and $Ni(CO)_x^-$ species.

$$CO\cdots CO + e^- \rightarrow (CO)_2^- \quad (5)$$

The CCl_4 molecule is well-known[27] for its high electron capture cross-section and the resulting dissociative capture process giving CCl_3 and Cl^-. Hence, during sample condensation in excess argon, CCl_4 will dominate electron capture reactions and minimize the formation of other anions through reaction 6. The absence of anion absorptions in the CCl_4-doped experiment is explained accordingly. The same effect has been found in other laser-ablation experiments with Fe and carbon monoxide.[19] As observed earlier,[25] full arc photolysis photodetaches Cl^- and provides electrons for the neutralization of CCl_3^+ and growth of CCl_3 on photolysis, also observed here.

$$CCl_4 + e^- \rightarrow CCl_3 + Cl^- \quad (6)$$

Conclusions

Laser-ablation of Ni metal coupled with matrix isolation produces and traps the neutral $Ni(CO)_{1-4}$ molecules and the stable $Ni(CO)_{1-3}^-$ molecular anions that are identified from isotopic substitution, photolysis behavior, and DFT frequency calculations. Six of these C−O stretching fundamentals are predicted within an average of 14 cm^{-1} by DFT/BP86 frequency calculations, the anions just as accurately as the neutral complexes. In particular, the intricacies of carbon 12/13 and oxygen 16/18 isotopic ratios for the NiCO and $NiCO^-$ monocarbonyls and both symmetric and antisymmetric C−O stretching modes of $Ni(CO)_2$ and the antisymmetric vibrations of $Ni(CO)_{2,3}^-$ provide a description of the normal modes, which are accurately matched by the DFT frequency calculations. Finally, it appears that CCl_4 doping provides a diagnostic for molecular anions by eliminating them from the product spectrum owing to preferential electron capture by CCl_4.

Acknowledgment. We thank the National Science Foundation (CHE97-00116) for financial support and L. Manceron for unpublished spectra in the 1800 cm^{-1} region.

JA9820644

(22) Jacox, M. E.; Milligan, D. E. *J. Chem. Phys.* **1965**, *43*, 866.
(23) Andrews, L. *J. Chem. Phys.* **1986**, *48*, 972.
(24) Jacox, M. E.; Milligan, D. E. *J. Chem. Phys.* **1971**, *54*, 3935.
(25) Prochaska, F. T.; Andrews, L. *J. Chem. Phys.* **1977**, *67*, 1091 and references therein.
(26) Maier, G.; Reisenauer, H. P.; Hu, J.; Hess, B. A., Jr.; Schaad, L. J. *Tetrahedron Lett.* **1989**, *30*, 4105.
(27) Illenberger, E. *Ber. Bunsenges. Phys. Chem* **1982**, *86*, 252. Matejcik, S.; Kiendler, A.; Stamatovic, A.; Märk, T. D. *Int. J. Mass. Spectrom. Ion Proc.* **1995**, *149/150*, 311.